TREM2 Variants as A Possible Cause of Frontotemporal Dementia with Distinct Neuroimaging Features

Short Title: Clinical Features of Pathogenic *TREM2* Variants

Bedia Samanci[1], MD, Başar Bilgiç[1], MD, Özlem Gelişin[1, #a], MD, Fatih Tepgeç[2], PhD, Gamze Guven[3], PhD, Zeynep Tüfekçioğlu[1], MD, Merve Alaylıoğlu[4], PhD, Hasmet A. Hanagasi[1], MD, Hakan Gürvit[1], MD, Rita Guerreiro[5], PhD, John Hardy[6], PhD, Murat Emre[1], MD

[1]Behavioral Neurology and Movement Disorders Unit, Department of Neurology, Istanbul Faculty of Medicine, Istanbul University, Istanbul, Turkey.

[2]Department of Medical Genetics, Istanbul Faculty of Medicine, Istanbul University, Istanbul, Turkey.

[3]Department of Genetics, Aziz Sancar Institute of Experimental Medicine, Istanbul University, Istanbul, Turkey.

[4]Department of Medical Biology, Cerrahpasa Faculty of Medicine, Istanbul University-Cerrahpasa, Istanbul, Turkey.

[5]Center for Neurodegenerative Science, Van Andel Institute, Grand Rapids, Michigan, USA.

[6]Department of Neurodegenerative Disorders, Institute of Neurology, University College London, London, UK.

[#a] Current Address: Department of Neurology, Faculty of Medicine, Bezmialem University, Istanbul, Turkey.

Corresponding author: Başar Bilgiç, MD

Address: Behavioral Neurology and Movement Disorders Unit, Department of Neurology, Istanbul Faculty of Medicine, Istanbul University, Istanbul, Turkey

Phone: +90 212 414 2000

E-mail: bilgicb@gmail.com

Word count of the main manuscript: 3471

1

2   DR. BEDIA SAMANCI (Orcid ID : 0000-0003-0667-2329)

3   DR. BASAR BILGIC (Orcid ID : 0000-0001-6032-0856)

4   MISS ZEYNEP TUFEKCIOGLU (Orcid ID : 0000-0001-6989-8611)

5   DR. HAKAN GURVIT (Orcid ID : 0000-0003-2908-8475)

6

7

8   Article type   : Original Article

9

10

11 **ABSTRACT**

12 **Background**: Nasu-Hakola disease (NHD) is a rare, autosomal recessive disorder
13 characterized by skeletal and neurological symptoms. Behavioral symptoms with cognitive
14 impairment may mimic the behavioral variant of frontotemporal dementia (bvFTD) and other
15 early-onset dementias. We analyzed our patients and reviewed the literature to delineate
16 neurological and neuroimaging findings suggestive of NHD.

17 **Method:** Fourteen patients carrying a pathogenic mutation in the *TREM2* gene were found in
18 our database. Demographic, clinical, laboratory, radiological data were retrieved and
19 analyzed.

20 **Results**: Presenting clinical picture was behavioral changes with cognitive decline
21 resembling bvFTD in all patients. The mean age was 37.1±4.97 years, the mean duration of
22 the disease was 8.9±3.51 years. Only two patients had typical bone cysts. Seven patients had
23 bilateral calcification of the basal ganglia in the computerized tomography of the brain.
24 Magnetic resonance imaging (MRI) of the brain revealed severe atrophy of the corpus
25 callosum, enlargement of the ventricles, atrophy of the caudate nuclei, periventricular white
26 matter changes in all patients. Symmetrical global atrophy of the brain, mainly affecting
27 frontoparietal and lateral temporal regions were observed in all cases, and 13 patients had
28 atrophy of hippocampus. Cerebrospinal fluid examination of ten patients showed elevated
29 protein levels in six and the presence of oligoclonal bands in four patients.

30 **Conclusion:** A combination of white matter changes, enlarged ventricles, atrophy of caudate
31 nuclei, thinning of the corpus callosum in MRI strongly suggests NHD in patients with FTD

1 syndrome. Molecular genetic analysis should be performed in suspected cases, and families

2 should receive genetic counseling.

3 **Keywords:** Nasu-Hakola disease, behavioral variant of frontotemporal dementia,

4 neuroimaging, genetic analysis, *TREM2*.

5

6

7

8 **INTRODUCTION**

9 Nasu-Hakola disease (NHD), also known as polycystic lipomembranous osteodysplasia with

10 sclerosing leukoencephalopathy (PLOSL), is a rare, autosomal recessive disorder of the

11 skeletal and nervous system, characterized by multifocal bone cysts, early-onset dementia

12 with a frontal lobe syndrome. The first cases with autopsy findings were published by Nasu

13 and Hakola [1, 2], and the course of the disease was divided into four stages: a) latent, b)

14 osseous, c) early neurologic, and d) late neurologic. Patients in the late stage usually die by

15 the age of 50 years [1, 3]. Mutations in two genes, triggering receptor expressed on myeloid

16 cells-2 (*TREM2*) [4-15] (**Supplementary Table**) and tyrosine kinase-binding protein

17 (*TYROB*, also known as *DAP12*), have been associated with NHD.

18 Clinical manifestation of NHD may present with the involvement of the central nervous

19 system (CNS) in the absence of characteristic skeletal symptoms [5, 9]. CNS symptoms are

20 usually cognitive decline and behavioral changes, resembling behavioral variant

21 frontotemporal dementia (bvFTD) [10, 15]. Although FTD, other early-onset dementia

22 diseases, and NHD may share common clinical symptoms, it is critical to differentiate these

23 disorders as management and genetic approach substantially vary in these diseases. There

24 have been a few case series regarding neuroimaging findings in NHD patients, but less is

25 known in patients with neurological onset. Herein, we describe clinical and neuroimaging

26 characteristics of fourteen cases carrying *TREM2* gene mutations presented with neurological

27 symptoms and twelve of whom had no joint pain or characteristic bone cysts in our series.

28

29 **METHOD**

30

31 **Patient Selection, Clinical and Laboratory Evaluations**

1   NHD patients were identified from the database of the Behavioral Neurology and Movement

2   Disorders Unit of Istanbul University including 10080 patients from November 1, 1999,

3   through January 1, 2010. Forty three of 390 dementia patients with bvFTD phenotype were

4   screened for *TREM2* and *DAP12* gene mutations for possible NHD, and 14 patients, who

5   admitted to our clinic between 2006 and 2020, with a genetically confirmed diagnosis of

6   NHD were included in this study. The estimated prevalence of these mutations was 0.14%.

7   All patients had agreed to genetic analysis at the time of initial clinical evaluation, and their

8   blood samples were analyzed for mutations in *TREM2* and *DAP12* genes.

9   Demographic data and clinical parameters including somatic neurological findings, mental

10   state examination, X-ray of extremities, and cerebrospinal fluid (CSF) exam including cell

11   count, biochemistry, oligoclonal band (OCB) patterns, and amyloid-beta 1-42,

12   phosphorylated tau, and total tau levels were analyzed. X-rays of the lower extremities of the

13   patients (except for the patients with bone cysts) were evaluated for cortical thickness index

14   (CTI) to show whether there was asymptomatic bone involvement. CTI was defined as the

15   ratio of the femoral diaphyseal diameter (outer diameter) minus the intramedullary canal

16   diameter (inner diameter) to the femoral diaphyseal diameter. These diameters were

17   measured 10 cm below the midpoint of the lesser trochanter [16].

18   **Evaluation of Neuroimaging Findings**

19   Brain computed tomography (CT) and MRI scans had been performed at the time of

20   diagnosis and were re-analyzed. All CT scans were evaluated for the presence of

21   calcification, and MRI scans were evaluated for cerebral atrophy pattern, quantitative

22   analysis of hippocampal atrophy [17], and white matter changes.

23   Fluorodeoxyglucose - positron emission tomography (FDG-PET) scans were available for

24   three patients, and these were evaluated for metabolic changes.

25   **Standard Protocol Approvals, Registrations, and Patient Consents**

26   This retrospective study with prospectively managed data was authorized by the local

27   institutional review board (IRB: 26.02.2021-94695). All procedures performed in studies

28   involving human participants were in accordance with the ethical standards of the

29   institutional and/or national research committee and with the 1964 Helsinki declaration and

1 its later amendments or comparable ethical standards. Informed consent forms for genetic

2 analysis and consent to publish were obtained from all participants.

3 **RESULTS**

4 **Clinical and Laboratory Findings**

5 Seven male and seven female NHD patients carrying a pathogenic mutation in *TREM2* were

6 included in the study. There was no patient with a pathogenic mutation in the *DAP12* gene in

7 our database. The mean age was 37.1 ± 4.97 years (range: 31-45 years), and the mean age of

8 onset was 33 ± 5.29 years (range: 20-39 years). Mean disease duration was 8.9 ± 3.51 years

9 (range: 4-13 years), and the mean duration of follow-up was 5.6 ± 3.16 years (range: 2-12

10 years).

11 None of the female patients had alopecia, and two male patients had male-pattern hair loss

12 (P7 and P13). Bilateral optic atrophy was detected in the ophthalmological evaluation in one

13 patient (P7) who had no visual complaints and had normal visual acuity. The parents of all

14 patients, except for two siblings, had consanguineous marriages.

15 All 14 patients had presented with behavioral symptoms along with a dysexecutive syndrome

16 fulfilling the criteria for "possible" bvFTD [18]. Seizures were present in 9 patients and

17 preceded the onset of dementia symptoms in two patients (**Table 1**, P3, and P14), who were

18 not diagnosed at the time of seizures. All patients had an akinetic-rigid syndrome leading to

19 severe disability, which did not respond to L-dopa or dopamine agonists. Two patients who

20 had homozygous p.D86V mutations had bone cysts detected in routine screening, and one of

21 them had a history of bone fracture**.** The median value of CTI in patients without detectable

22 bone cysts was 0.65 (range: 0.61-0.67) (**Supplementary Figure**).

23 Demographic, clinical, and genetic features [19] are presented in **Table 1**.

Table 1. Clinical, demographic, and genetic features of the patients with Nasu-Hakola disease.

Patient ID	Gender	Age of onset	Presentation	Family history	Epileptic seizures	Fracture history/ Bone cysts	Parkinsonism	Disease duration /Status	Mutation	Pathogenicity[&]
P1 [a]	M	20	bvFTD-like	No	+	-/-	+	13 years, Dead	Homozygous p.Q33X	Pathogenic
P2	M	35	bvFTD-like	No	+	-/+ (Bilateral talus)	+	5 years, Dead	Homozygous p.D86V	Pathogenic
P3* [a]	F	40	bvFTD-like	Yes*	+	-/-	+	9 years, Alive	Compound heterozygous p.[(Y38C)];[(D86)]	Pathogenic
P4* [a]	F	30	bvFTD-like	Yes*	+	-/-	+	13 years, Dead	Compound heterozygous p.[(Y38C)];[(D86)]	Pathogenic
P5	F	35	bvFTD-like	No	+	+/+ (Bilateral humerus)	+	10 years, Alive	Homozygous p.D86V	Likely Pathogenic
P6	F	25	bvFTD-like	No	+	-/-	+	12 years, Alive	Homozygous p.Y38C	Pathogenic
P7	M	36	bvFTD-like	No	-	-/-	+	4 years, Alive	Homozygous p.D86V	Likely Pathogenic

P8	F	38	bvFTD-like	Yes**	+	-/-	+	11 years, Alive	Homozygous p.D86V	Likely Pathogenic
P9	F	33	bvFTD-like	No	-	+/-	+	4 years, Alive	Homozygous p.D86V	Likely Pathogenic
P10	F	33	bvFTD-like	Yes***	-	-/-	+	6 years, Alive	Homozygous p.T66M	Pathogenic
P11	M	31	bvFTD-like	No	-	-/-	+	4 years, Alive	Homozygous D119Efs70	Pathogenic
P12 [a]	M	39	bvFTD-like	No	-	-/-	+	11 years, Dead	Homozygous p.T66M	Pathogenic
P13	M	35	bvFTD-like	No	+	-/-	+	10 years, Dead	Homozygous p.T66M	Pathogenic
P14 [a]	M	33	bvFTD-like	No	+	-/-	+	12 years, Dead	Homozygous p.Y38C	Pathogenic

M: Male, F: Female, bvFTD: Behavioral variant of frontotemporal dementia. *Siblings. **Her sister was reported to have similar clinical features, but she had died without spesific diagnosis. ***Her brother was reported to have similar clinical features, but he had died without spesific diagnosis.

[a] The detailed clinical and laboratory features of the patients P1, P3, P4, P12, and P14 were reported in separate publications [9, 10].

&Pathogenicity of the variants were determined according to ACMG 2015 criteria [19].

1 Ten patients underwent lumbar puncture. One had CSF mild pleocytosis (10
2 lymphocytes/mm3), protein levels were above the normal limits (>45 mg/dL) in 6 patients.
3 Patterns of OCBs were as follows: six patients had pattern 1 (no bands in CSF and serum),
4 two had pattern 3 (OCBs in CSF and identical OCBs in serum and CSF), and two had pattern
5 4 (identical pattern of OCBs in CSF and serum). The patient with CSF pleocytosis had
6 elevated CSF protein levels with positive OCB (pattern 3). After corticosteroid and
7 intravenous immunoglobulin treatment for possible autoimmune encephalitis in this patient,
8 CSF cell count returned to normal, and OCB pattern reverted to pattern 1 without clinical
9 benefit. CSF amyloid-beta 1-42, phosphorylated tau, and total tau levels were available for
10 two patients showing increased tau levels with normal amyloid beta concentrations. Detailed
11 CSF results of the patients are shown in **Table 2.**

12 **Table 2.** Cerebrospinal fluid (CSF) analysis of the patients who underwent lumbar puncture.

Patient ID	Pleocytosis	Protein level (mg/dl)	OCB pattern	CSF amyloid-beta 1-42 (pg/ml)	CSF phosphorylated tau (pg/ml)	CSF total tau (pg/ml)
P1	No	N/A	*1*	N/A	N/A	N/A
P2	No	*25,7*	*1*	N/A	N/A	N/A
P3	*10 lymphocytes/mm3*	*51*	*3*	N/A	N/A	N/A
P5	No	*75*	*1*	N/A	N/A	N/A
P6	No	*26*	*1*	N/A	N/A	N/A
P7	No	*45*	*1*	*1544*	*80*	*795*
P10	No	*41,8*	*4*	N/A	N/A	N/A
P11	No	*71*	*1*	*1460*	*42*	*423*
P12	No	*67,8*	*4*	N/A	N/A	N/A
P13	No	*57,2*	*3*	N/A	N/A	N/A

13 OCB: Oligoclonal band, CSF: Cerebrospinal fluid, N/A: Not available.

14

1   During the clinical follow-up period, the father of patients P3 and P4, and the father of patient

2   P5 developed Parkinson's disease, and the father of patient P6 developed Alzheimer's disease

3   (AD) in his early 60s. In 2020, patient P7 had test-proven COVID-19 disease with mild

4   symptoms, including fever and cough, which were recovered in two days.

5

6   **Neuroimaging Features**

7   Brain CT scans performed after a mean period of 4.8 ± 3.19 years following initial symptoms

8   were available in thirteen patients. Seven had bilateral calcification of the basal ganglia.

9   Calcifications were mostly restricted and not as widespread as seen in Fahr's disease.

10   MRI scans performed after a mean period of 4.9 ± 3.36 years following initial symptoms

11   revealed significant thinning of the corpus callosum and marked enlargement of the lateral

12   and third ventricles in all patients. None of the patients had dilated fourth ventricle or stenosis

13   of the aqueduct. Thinning of the corpus callosum was diffuse in all subjects, although

14   splenium was relatively spared **(Figure 1).** Global atrophy of the brain, predominantly

15   involving frontoparietal and lateral temporal areas and bilateral atrophy of the caudate nuclei

16   were present in all patients and thirteen of the patients had also atrophy of the hippocampus

17   to various degrees. All patients had diffuse, confluent white matter lesions that were mildly

18   hyperintense on T2-weighted and fluid-attenuated inversion recovery (FLAIR) sequences.

19   These white matter abnormalities were more prominent in the areas adjacent to the anterior

20   and posterior horns of the lateral ventricles. Neuroimaging features of the patients are

21   presented in **Table 3**. There was a follow-up MRI scan in four patients after a mean period of

22   2.3 ± 1.89 years. In contrast to the marked progression of cortical atrophy, a notably slow

23   progression of white matter involvement was observed in one patient with a radiological

24   follow-up of 5 years (**Figure 2**). No significant progression was detected in the white matter

25   and corpus callosum of the other three patients who had a radiological follow-up interval of

26   less than 2 years. Four patients with calcification in their CT scan had consecutive CT scans

27   after a mean period of 2.8 ± 1.71 years, and no progression was observed in the number and

28   size of the calcifications **(Figure 3)**. No different pattern of neuroradiological findings were

29   observed in patients with bone lesions.

30

1   Three patients had brain FDG-PET scans, which showed widespread cortical
2   hypometabolism, including basal ganglia (see **Table 3 for details).**

Table 3. Neuroimaging findings of the patients.

Patient ID	Thinning of the CC*	WM involvement	Ventricular dilatation	Cortical atrophy	Hippocampal atrophy (MTA score)	FDG-PET	Calcification on CT
P1	+	+	*Lateral ventricle:* + *3rd ventricle:* + 4th ventricle: -	Frontal (more prominent), parietotemporal, perisylvian, caudate	3	N/A	No
P2	+	+	*Lateral ventricle:* + 3rd ventricle: + 4th ventricle: -	Frontoparietal, perisylvian, caudate	2	N/A	Yes
P3	+	+	*Lateral ventricle:* + *3rd ventricle:* + 4th ventricle: -	Frontotemporoparietal, perisylvian, caudate	3	N/A	Yes
P4	+	+	*Lateral ventricle:* + 3rd ventricle: + 4th ventricle: -	Global, caudate	3	N/A	No
P5	+	+	*Lateral ventricle:* + 3rd ventricle: + 4th ventricle: -	Frontoparietal, perisylvian, caudate	3	N/A	Yes
P6	+	+	*Lateral ventricle:* + 3rd ventricle: + 4th ventricle: -	Frontal, caudate	2	Hypometabolism in bilateral frontal, parietal, posterior cingulate, left anterior and lateral temporal, bilateral basal ganglia and thalamus	Yes
P7	+	+	*Lateral ventricle:* + 3rd ventricle: + 4th ventricle: -	Parietal (more prominent), frontal, perisylvian, caudate	2	Hypometabolism in right frontal, bilateral parietal, anterior temporal, right basal ganglia	Yes

P8	+	+	*Lateral ventricle:* + 3rd ventricle: + 4th ventricle: -	Frontotemporal (more prominent), global, caudate	3	N/A	Yes
P9	+	+	*Lateral ventricle:* + 3rd ventricle: + 4th ventricle: -	Parietal (more prominent), frontal, perisylvian, caudate	2	Hypometabolism in bilateral parietal, left anterior temporal, right basal ganglia	No
P10	+	+	*Lateral ventricle:* + 3rd ventricle: + 4th ventricle: -	Global, caudate	2	N/A	Yes
P11	+	+	*Lateral ventricle:* + 3rd ventricle: + 4th ventricle: -	Frontoparietal (more prominent), global, perisylvian, caudate	1	N/A	No
P12	+	+	*Lateral ventricle:* + *3rd ventricle:* + 4th ventricle: -	Frontal (more prominent), global, caudate	3	N/A	N/A (No sign of calcification on the MRI)
P13	+	+	*Lateral ventricle:* + *3rd ventricle:* + 4th ventricle: -	Frontal (more prominent), perisylvian, caudate	3	N/A	No
P14	+	+	*Lateral ventricle:* + *3rd ventricle:* + 4th ventricle: -	Frontal (more prominent), global, caudate	2	N/A	No

CC: Corpus callosum, WM: White matter, MTA: Medial temporal atrophy, FDG-PET: Fluorodeoxyglucose - positron emission tomography, CT: Computed tomography.

*Marked atrophy in CC in the 1/3 anterior and 1/3 medial, and less atrophy in the 1/3 posterior area.

DISCUSSION

Traditionally, the clinical course of NHD has been divided into four stages: (a) latent, (b) osseous, (c) early neurological, and (d) late neurological [1, 3]. Patients in our series presented with neurological symptoms. Only two had bone cysts in their routine diagnostic workup, and one of them had a history of bone fracture. Our study consisting of 14 NHD patients is the largest case series published to date, and all our patients were admitted to memory clinic with symptoms of early-onset dementia. We did not detect any skeletal deformity in one patient with prior bone fracture, which was attributed to a fall. Our findings put into question the traditional clinical concept of disease progression in NHD.

Differential diagnosis of patients with early-onset dementia can be challenging. Underlying pathology can be a common neurodegenerative disease such as AD or frontotemporal dementia as well as rare diseases like NHD. Diagnosis may necessitate extensive diagnostic workup. Characteristic neuroimaging findings detectable in routine MRI can aid the diagnosis, as is the case for NHD. Our data revealed that all fourteen NHD patients with neurological onset had four common neuroimaging findings in MRI: (a) thinning of the corpus callosum, (b) diffuse periventricular white matter abnormalities, (c) atrophy of caudate nuclei, and (d) enlargement of the lateral and third ventricles with sparing of the fourth ventricle. Although all our patients had diffuse cortical atrophy mainly in the frontoparietal and temporal regions, no specific atrophy pattern was observed. Consistent with the postmortem histopathological studies in NHD [20], various degree of hippocampal atrophy was evident in the MRI in the majority of patients. Approximately half of the patients exhibited calcifications in the basal ganglia, constituting a suggestive but not pathognomonic finding for NHD.

Although the clinical course of NHD follows a classical pattern with early and late neurological symptoms following osseous symptoms, all the patients in our cohort presented with neurological symptoms. This finding is contrary to majority of previous studies and the underlying factors remain largely unknown. Neurological presentation of NHD in our series consisted of early-onset dementia with personality changes, progressive behavioral symptoms, and subsequent cognitive impairment, resembling FTD. As the differential diagnosis of these two diseases is essential, the presence of seizures, which is unusual in FTD, maybe a hint for NHD. Two of our patients had a history of epileptic seizures before the onset of other symptoms, and seven patients developed seizures after the onset of

dementia symptoms. Another different clinical aspect of NHD compared to FTD seems the age of onset of dementia symptoms. While the age of onset in majority of the FTD patients was between 45-65 or even more [21], all of NHD patients in our series developed the disease before the age of 41. Also, neuroimaging findings are very helpful to differentiate NHD from bvFTD. Thinning of the corpus callosum with calcifications in basal ganglia make the diagnosis of FTD unlikely, some FTD patients may have white matter changes, ventricular dilatation, and atrophy of the caudate nuclei. Even some FTD patients carrying mutations in the progranulin gene may have significant white matter hyperintensities in the MRI, the presence of confluent white matter hyperintensities in FTD is rare [22, 23]. Patients with adult-onset leukoencephalopathy with axonal spheroids and pigmented glia (ALSP) usually have thinning of the corpus callosum, calcifications, and white matter changes. Calcifications in ALSP, however, tend to be located in the periventricular white matter, whereas they tend to be confined to basal ganglia in NHD. White matter changes in FLAIR and T2-weighted images are likely to be more intense in NHD compared to ALSP [24].

Neuroimaging findings in NHD have been described previously in several case reports. Diffuse cortical atrophy, ventricular enlargement, and calcification without white matter changes were described in one patient [25]. In another report, ventricular enlargement and white matter abnormalities were described in MRI [26]. Two infantile NHD patients from Tunisia with both skeletal and CNS involvement were reported to have ventricular dilatation and thinning of the corpus callosum [27]. In a case series including eight NHD patients with skeletal and neurological symptoms, ventricular enlargement was present in all, and five patients had diffuse white matter hyperintensities [3]. In several reports including NHD patients with symptomatic or asymptomatic bone cysts, three of the four common neuroimaging findings found in the current study were described, including thinning of the corpus callosum, ventricular enlargement, and white matter changes [28-31]. A limited number of case reports described neuroimaging findings in NHD patients presented with neurological symptoms [5, 9, 32, 33], three findings mentioned above were present in all these cases. Regarding all the reported patients in these papers, only 11 (including 3 patients in the present study) of 32 patients were reported to lack characteristic bone lesions. Contrary to this, majority of the patients (86%) in our series had no characteristics skeletal lesions. Also, the median CTI value, which is a radiological (X-ray) marker for bone mineral density, was found to be over the threshold values determined in the age 50 years and over population for osteoporosis and fracture risk reported as 0.56 and 0.62, respectively [34]. Although we

had no chance to compare the CTI values of NHD patients with age-matched control subjects, increased age is known to be associated with thinner cortex of the femoral bone [35, 36]. Therefore, CTI values in relatively young NHD patients may still represent a pathological state. In line with this assumption, one of our patients had suffered from bone fracture even she had no cystic bone lesion and with normal CTI values. It is unfortunate that our study is limited by the lack of more detailed techniques such as bone density scan (DXA) and MRI or CT for extremities to further analyze the presence of skeletal abnormalities in NHD patients.

There may be a wide spectrum of skeletal involvement in NHD, ranging from asymptomatic bone mineral density deficits to characteristic bone cysts leading to pathological fractures. *TREM2* signaling remains poorly understood and receptor-ligand interactions are complex as there are a variety of ligands of *TREM2* receptor such as lipoproteins (low-density lipoprotein) and apolipoproteins (APOE), and bacterial anionic molecules [37, 38]. Activation and regulation of the *TREM2* pathway is also a complex process critically dependent on tissue context and intracellular state. At a cellular level, *TREM2* signaling in various contexts induces significant changes in cellular phenotypes and functions, which seems to be a consequence of several *TREM2*-dependent processes, including induction of phagocytosis, lipid metabolism, and metabolic shift, promoting cell survival and counteracting inflammatory activation [39]. The complex nature of the *TREM2* pathway and possible other genetic and epigenetic interactions may be the underlying cause of phenotypic variations especially in the skeletal system in NHD patients as seen in the five patients in the current study whom carrying same homozygous p.D86V mutation but only the two of them showed characteristic bone cysts.

Neuroimaging findings may be an early feature of NHD and may be present in asymptomatic cases. White matter changes, atrophy of the brain, thinning of the corpus callosum, and calcification in the basal ganglia became evident before the onset of cognitive decline and behavioral symptoms in patients with skeletal involvement only [40]. Less is known about the course of the neuroimaging findings, and our study suggests a relatively slow progression of white matter involvement in contrast to the gradual atrophy of the cortical areas after the disease onset. Our data also point out a stable nature of calcifications if present.

There are few case reports on FDG-PET and SPECT findings in NHD patients, which described global hypometabolism or hypoperfusion in the cortex and basal ganglia [31, 41-43]. FDG-PET was available in three of our patients, and all had hypometabolism in basal ganglia and parietal lobe as well as hypometabolism in various cortical areas. Although Ghezzi et al reported the presence of amyloid accumulation shown by amyloid PET imaging with decreased CSF amyloid level in one NHD case carrying the homozygous mutation (Q33X) in *TREM2* gene [29], this was not confirmed in two other patients, who had c.391+1G>A and R47C mutations, respectively [28, 44]. Recently Maderna et al. [45] has reported the neuropathologic findings of a patient who was carrying the same Q33X mutation and the patient showed neuropathological findings consistent with both NHD and AD. In our study, CSF biomarker analysis was available for two patients, and none had decreased amyloid-beta levels compatible with the findings as reported by Ghezzi et al [29]. Type of mutation may be the underlying cause of concomitant amyloid deposition in NHD patients, however, several questions on the deposition of amyloid in NHD patients remain to be answered, and considerably more work will need to be done to determine the presence of ongoing pathological depositions in NHD patients.

The main pathological finding underlying MRI findings in NHD is sclerosing leukoencephalopathy. Postmortem examination in eight patients revealed marked atrophy of the white matter, loss of myelin sheaths, and nerve fibers with prominent gliosis [46]. Immunochemistry showed leakage of plasma proteins into the parenchyma and increased vascular density in the white matter, small vessel walls also appeared thickened. Recent immunohistochemical studies revealed diffuse microglial activation and inflammation in the white matter. This is not surprising as *TREM2* is expressed on microglia [47], it modulates the activation of microglia as well as microglia-mediated inflammatory responses [20, 48], and modulation of phagocytosis [49, 50]. Impairment in tissue debris removal by microglial cells and accompanying proinflammatory state might be the main pathophysiology in *TREM2* mutations [28, 51]. Possibly indicating inflammatory process in the CNS, elevated CSF protein was found in six, and OCBs were present in four patients. The presence of OCBs was reported in a few previous studies [33, 52]. Furthermore, Errichiello et al. [30] hypothesized that defined as a multisystem immunological disorder, anti-inflammatory medications, or repositioning/repurposing of myeloid-specific compounds might be effective in the early stages of NHD to prevent progressive neurodegeneration. One of our patients with pleocytosis elevated CSF protein, and OCB positivity did not benefit from corticosteroid and

intravenous immunoglobulin treatments in the first year of the disease. This observation may suggest the ineffectiveness of corticosteroid and intravenous immunoglobulin treatments when initiated after the onset of neurological symptoms. However, these treatments may still have the potential to slow down neurodegeneration if initiated before the onset of neurological symptoms. Interventions on asymptomatic mutation carriers or patients diagnosed in the osseous stage would help to establish a higher degree of accuracy on this matter.

In our study, all of the patients had extrapyramidal signs, and two of the living fathers of the patients developed typical Parkinson's disease during follow-up. Deficiencies of both *TREM2* and *DAP12* have been shown to significantly affect microglial activity in various types of neural diseases, including Parkinson's disease [53, 54]. These disorders may share common pathways centered on microglial function in which *TREM2* seems to have a pivotal role. It is possible that the degree of *TREM2* protein defect and consequently microglial dysfunction or survival as well as the regional variations in microglial density and the localization of the defective inflammatory processes within the CNS may contribute to the different clinical phenotypes [54, 55].

There are several limitations to our study. Firstly, although we had the largest number of patients ever reported, the sample size is still small, studies with larger sample size are needed to confirm our findings. Secondly, no postmortem examination was available to reveal the underlying pathophysiology. Thirdly, PET imaging, and CSF analysis were performed only in a few patients. Additionally, only X-rays were used to evaluate the asymptomatic cystic bone lesions. CT scan or MRI, dual energy X-ray absorptiometry (DXA) can be better further imaging modalities in suspected patients.

In conclusion, neuroimaging findings consisting of thinning of the corpus callosum, ventricular enlargement, dilatation of the lateral ventricle, atrophy of the caudate nuclei, and periventricular white matter changes suggest a diagnosis of NHD and are useful in the differential diagnosis of early-onset dementias, particularly FTD. Pathological studies suggest vascular and inflammatory processes predominantly involving the white matter are responsible for these neuroradiological findings. Since NHD is an autosomal recessively inherited disorder, genetic analysis should be performed as a first-line investigation in suspected cases, especially in countries where there is a high rate of consanguineous

marriages. This result broadens the clinical spectrum associated with *TREM2* mutations, which should be considered in patients with early-onset dementia with leuko-encephalopathy, and atrophy even in the absence of symptomatic skeletal symptoms.

Acknowledgment

The authors would like to thank the patients for their generous participations.

Funding

No support has been received for this study.

Disclosure of Conflict of Interest

The authors report no financial or other conflicts of interest.

Data Availability Statement

The data that support the findings of this study are available from the corresponding author upon reasonable request.

Author Contribution

BS: Conceptualization, data curation, formal analysis, investigation, methodology, resources, writing-original draft; BB: Conceptualization, data curation, formal analysis, investigation, methodology, resources, supervision, writing-original draft and review§editing; ÖG: data curation, investigation, writing- review§editing; FT: formal analysis, investigation, methodology, writing- review§editing; GG: formal analysis, investigation, methodology, writing- review§editing; ZT: data curation, investigation, writing- review§editing; MA: formal analysis, methodology, writing- review§editing; HAH: data curation, investigation, supervision, writing- review§editing; HG: data curation, investigation, writing- review§editing; RG: formal analysis, investigation, methodology, writing-review§editing; JH: formal analysis, investigation, methodology, writing-review§editing; ME: Conceptualization, methodology, supervision, writing-original draft and review§editing. All authors read and approved the final manuscript.

REFERENCES:

[1].   Hakola HP. Neuropsychiatric and genetic aspects of a new hereditary disease characterized by progressive dementia and lipomembranous polycystic osteodysplasia. *Acta Psychiatr Scand Suppl*. 1972 **232:** 1-173.

[2].   Nasu T, Tsukahara Y, Terayama K. A lipid metabolic disease-"membranous lipodystrophy"-an autopsy case demonstrating numerous peculiar membrane-structures composed of compound lipid in bone and bone marrow and various adipose tissues. *Acta Pathol Jpn*. 1973 **23:** 539-558.

[3].   Paloneva J, Autti T, Raininko R*, et al.* CNS manifestations of Nasu-Hakola disease: a frontal dementia with bone cysts. *Neurology*. 2001 **56:** 1552-1558.

[4].   Paloneva J, Manninen T, Christman G*, et al.* Mutations in two genes encoding different subunits of a receptor signaling complex result in an identical disease phenotype. *Am J Hum Genet*. 2002 **71:** 656-662.

[5].   Chouery E, Delague V, Bergougnoux A, Koussa S, Serre JL, Megarbane A. Mutations in TREM2 lead to pure early-onset dementia without bone cysts. *Hum Mutat*. 2008 **29:** E194-204.

[6].   Bock V, Botturi A, Gaviani P*, et al.* Polycystic Lipomembranous Osteodysplasia with Sclerosing Leukoencephalopathy (PLOSL): a new report of an Italian woman and review of the literature. *J Neurol Sci*. 2013 **326:** 115-119.

[7].   Klunemann HH, Ridha BH, Magy L*, et al.* The genetic causes of basal ganglia calcification, dementia, and bone cysts: DAP12 and TREM2. *Neurology*. 2005 **64:** 1502-1507.

[8].   Soragna D, Papi L, Ratti MT, Sestini R, Tupler R, Montalbetti L. An Italian family affected by Nasu-Hakola disease with a novel genetic mutation in the TREM2 gene. *J Neurol Neurosurg Psychiatry*. 2003 **74:** 825-826.

[9].   Guerreiro RJ, Lohmann E, Brás JM*, et al.* Using exome sequencing to reveal mutations in TREM2 presenting as a frontotemporal dementia-like syndrome without bone involvement. *JAMA Neurol*. 2013 **70:** 78-84.

[10].   Guerreiro R, Bilgic B, Guven G*, et al.* Novel compound heterozygous mutation in TREM2 found in a Turkish frontotemporal dementia-like family. *Neurobiol Aging*. 2013 **34:** 2890.e2891-2895.

[11].   Thelen M, Razquin C, Hernandez I*, et al.* Investigation of the role of rare TREM2 variants in frontotemporal dementia subtypes. *Neurobiol Aging*. 2014 **35:** 2657 e2613-2657 e2619.

[12].   Dardiotis E, Siokas V, Pantazi E*, et al.* A novel mutation in TREM2 gene causing Nasu-Hakola disease and review of the literature. *Neurobiol Aging*. 2017 **53:** 194 e113-194 e122.

[13]. Chee KY, Gaillard F, Velakoulis D, Ang CL, Chin LK, Ariffin R. A case of TREM2 mutation presenting with features of progressive non-fluent aphasia and without bone involvement. *Aust N Z J Psychiatry*. 2017 **51:** 1157-1158.

[14]. Numasawa Y, Yamaura C, Ishihara S*, et al.* Nasu-Hakola disease with a splicing mutation of TREM2 in a Japanese family. *Eur J Neurol*. 2011 **18:** 1179-1183.

[15]. Giraldo M, Lopera F, Siniard AL*, et al.* Variants in triggering receptor expressed on myeloid cells 2 are associated with both behavioral variant frontotemporal lobar degeneration and Alzheimer's disease. *Neurobiol Aging*. 2013 **34:** 2077 e2011-2078.

[16]. Dorr LD, Faugere MC, Mackel AM, Gruen TA, Bognar B, Malluche HH. Structural and Cellular Assessment of Bone Quality of Proximal Femur. *Bone*. 1993 **14:** 231-242.

[17]. Scheltens P, Leys D, Barkhof F*, et al.* Atrophy of medial temporal lobes on MRI in "probable" Alzheimer's disease and normal ageing: diagnostic value and neuropsychological correlates. *J Neurol Neurosurg Psychiatry*. 1992 **55:** 967-972.

[18]. Rascovsky K, Hodges JR, Knopman D*, et al.* Sensitivity of revised diagnostic criteria for the behavioural variant of frontotemporal dementia. *Brain*. 2011 **134:** 2456-2477.

[19]. Richards S, Aziz N, Bale S*, et al.* Standards and guidelines for the interpretation of sequence variants: a joint consensus recommendation of the American College of Medical Genetics and Genomics and the Association for Molecular Pathology. *Genetics in Medicine*. 2015 **17:** 405-424.

[20]. Oyanagi K, Kinoshita M, Suzuki-Kouyama E*, et al.* Adult onset leukoencephalopathy with axonal spheroids and pigmented glia (ALSP) and Nasu-Hakola disease: lesion staging and dynamic changes of axons and microglial subsets. *Brain Pathol*. 2017 **27:** 748-769.

[21]. Moore KM, Nicholas J, Grossman M*, et al.* Age at symptom onset and death and disease duration in genetic frontotemporal dementia: an international retrospective cohort study. *Lancet Neurology*. 2020 **19:** 145-156.

[22]. Sudre CH, Bocchetta M, Cash D*, et al.* White matter hyperintensities are seen only in GRN mutation carriers in the GENFI cohort. *Neuroimage-Clinical*. 2017 **15:** 171-180.

[23]. Caroppo P, Le Ber I, Camuzat A*, et al.* Extensive White Matter Involvement in Patients With Frontotemporal Lobar Degeneration Think Progranulin. *Jama Neurology*. 2014 **71:** 1562-1566.

[24]. Sundal C, Van Gerpen JA, Nicholson AM*, et al.* MRI characteristics and scoring in HDLS due to CSF1R gene mutations. *Neurology*. 2012 **79:** 566-574.

[25]. Maner F, Ipekcioglu D, Karamustafalioglu N*, et al.* The case of a 43-year old Turkish male patient with Nasu-Hakola disease. *Asian J Psychiatr*. 2013 **6:** 631-632.

[26]. Kilic SA, Oner AY, Yuce C, Ozlu IC. Imaging findings of Nasu-Hakola disease: a case report. *Clin Imaging*. 2012 **36:** 877-880.

[27].   Chaabane M, Larnaout A, Sebai R, Nagi S, Touibi S, Hentati F. Nasu-Hakola disease in two Tunisian siblings: new radiological findings. *Neuroradiology*. 2000 **42:** 375-378.

[28].   Li X, Sun Y, Gong L*, et al.* A novel homozygous mutation in TREM2 found in a Chinese early-onset dementia family with mild bone involvement. *Neurobiol Aging*. 2020 **86:** 201 e201-201 e207.

[29].   Ghezzi L, Carandini T, Arighi A*, et al.* Evidence of CNS beta-amyloid deposition in Nasu-Hakola disease due to the TREM2 Q33X mutation. *Neurology*. 2017 **89:** 2503-2505.

[30].   Errichiello E, Dardiotis E, Mannino F, Paloneva J, Mattina T, Zuffardi O. Phenotypic Expansion in Nasu-Hakola Disease: Immunological Findings in Three Patients and Proposal of a Unifying Pathogenic Hypothesis. *Front Immunol*. 2019 **10:** 1685.

[31].   Coomans C, Sieben A, Lammens M*, et al.* Early-onset dementia, leukoencephalopathy and brain calcifications: a clinical, imaging and pathological comparison of ALSP and PLOSL/Nasu Hakola disease. *Acta Neurol Belg*. 2018 **118:** 607-615.

[32].   Le Ber I, De Septenville A, Guerreiro R*, et al.* Homozygous TREM2 mutation in a family with atypical frontotemporal dementia. *Neurobiol Aging*. 2014 **35:** 2419 e2423-2419 e2425.

[33].   Salmaggi A, Maccagnano E, Musso A, Di Lena L, Paloneva J, Boiardi A. An Italian family with Nasu-Hakola disease. *J Neurol*. 2003 **250:** 878-880.

[34].   Nguyen BNT, Hoshino H, Togawa D, Matsuyama Y. Cortical Thickness Index of the Proximal Femur: A Radiographic Parameter for Preliminary Assessment of Bone Mineral Density and Osteoporosis Status in the Age 50 Years and Over Population. *Clinics in Orthopedic Surgery*. 2018 **10:** 149-156.

[35].   Poole KES, Mayhew PM, Rose CM*, et al.* Changing Structure of the Femoral Neck Across the Adult Female Lifespan. *Journal of Bone and Mineral Research*. 2010 **25:** 482-491.

[36].   Mayhew PM, Thomas CD, Clement JG*, et al.* Relation between age, femoral neck cortical stability, and hip fracture risk. *Lancet*. 2005 **366:** 129-135.

[37].   Hsieh CL, Koike M, Spusta SC*, et al.* A role for TREM2 ligands in the phagocytosis of apoptotic neuronal cells by microglia. *Journal of Neurochemistry*. 2009 **109:** 1144-1156.

[38].   Kober DL, Brett TJ. TREM2-Ligand Interactions in Health and Disease. *Journal of Molecular Biology*. 2017 **429:** 1607-1629.

[39].   Deczkowska A, Weiner A, Amit I. The Physiology, Pathology, and Potential Therapeutic Applications of the TREM2 Signaling Pathway. *Cell*. 2020 **181:** 1207-1217.

[40].   Brenner C, Speck-Martins CE, Brum JM, Lucato LT, Leite Cda C. Computed tomography and magnetic resonance imaging in the osseous phase of Nasu-Hakola disease. *Arq Neuropsiquiatr*. 2014 **72:** 646-647.

[41].   Montalbetti L, Ratti MT, Greco B, Aprile C, Moglia A, Soragna D. Neuropsychological tests and functional nuclear neuroimaging provide evidence of subclinical impairment in Nasu-Hakola disease heterozygotes. *Funct Neurol*. 2005 **20:** 71-75.

[42].   Nakamagoe K, Shioya A, Yamaguchi T*, et al.* A Japanese case with Nasu-Hakola disease of DAP12 gene mutation exhibiting precuneus hypoperfusion. *Intern Med*. 2011 **50:** 2839-2844.

[43].   Koseoglu E, Tepgec F, Yetkin MF*, et al.* Nasu Hakola Disease: A Rare Cause of Dementia and Cystic Bone Lesions, Report of a New Turkish Family. *Noro Psikiyatr Ars*. 2018 **55:** 98-102.

[44].   Ng ASL, Tan YJ, Yi Z*, et al.* Targeted exome sequencing reveals homozygous TREM2 R47C mutation presenting with behavioral variant frontotemporal dementia without bone involvement. *Neurobiol Aging*. 2018 **68:** 160 e115-160 e119.

[45].   Maderna E, Visona S, Bolcato V*, et al.* Neuropathological Alzheimer's Disease Lesions in Nasu-Hakola Disease with TREM2 Mutation: Atypical Distribution of Neurofibrillary Changes. *Journal of Alzheimers Disease*. 2021 **79:** 25-30.

[46].   Kalimo H, Sourander P, Jarvi O, Hakola P. Vascular changes and blood-brain barrier damage in the pathogenesis of polycystic lipomembranous osteodysplasia with sclerosing leukoencephalophy (membranous lipodystrophy). *Acta Neurol Scand*. 1994 **89:** 353-361.

[47].   Redaelli V, Salsano E, Colleoni L*, et al.* Frontotemporal Dementia and Chorea Associated with a Compound Heterozygous TREM2 Mutation. *J Alzheimers Dis*. 2018 **63:** 195-201.

[48].   Cantoni C, Bollman B, Licastro D*, et al.* TREM2 regulates microglial cell activation in response to demyelination in vivo. *Acta Neuropathol*. 2015 **129:** 429-447.

[49].   Xing J, Titus AR, Humphrey MB. The TREM2-DAP12 signaling pathway in Nasu-Hakola disease: a molecular genetics perspective. *Res Rep Biochem*. 2015 **5:** 89-100.

[50].   Zhong L, Zhang ZL, Li X*, et al.* TREM2/DAP12 Complex Regulates Inflammatory Responses in Microglia via the JNK Signaling Pathway. *Front Aging Neurosci*. 2017 **9:** 204.

[51].   Kleinberger G, Brendel M, Mracsko E*, et al.* The FTD-like syndrome causing TREM2 T66M mutation impairs microglia function, brain perfusion, and glucose metabolism. *EMBO J*. 2017 **36:** 1837-1853.

[52].   Williamson JC, Larner AJ. Behavioral Variant Frontotemporal Dementia-like Syndrome With Novel Heterozygous TREM2 Frameshift Mutation. *Alzheimer Dis Assoc Disord*. 2019 **33:** 75-76.

[53].   Kinugawa K, Monnet Y, Bechade C*, et al.* DAP12 and CD11b contribute to the microglial-induced death of dopaminergic neurons in vitro but not in vivo in the MPTP mouse model of Parkinson's disease. *Journal of Neuroinflammation*. 2013 **10**.

[54]. Rayaprolu S, Mullen B, Baker M*, et al.* TREM2 in neurodegeneration: evidence for association of the p.R47H variant with frontotemporal dementia and Parkinson's disease. *Molecular Neurodegeneration*. 2013 **8**.

[55]. Konishi H, Kiyama H. Non-pathological roles of microglial TREM2/DAP12: TREM2/DAP12 regulates the physiological functions of microglia from development to aging. *Neurochemistry International*. 2020 **141**.

1   **FIGURE LEGENDS**

2

3   **Figure 1.** An example of a normal corpus callosum (a), and thinning of the corpus callosum

4   in 13 patients (b). Thinning is diffuse, but splenium is relatively spared.
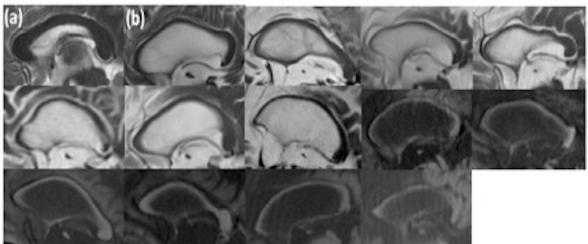
5

6   **Figure 2.** Course of cortical atrophy and white matter involvement in two patients. (a) CT

7   scans acquired in 2012 (left) and in 2017 (right) demonstrating the progressive atrophy of the

8   fronto-temporal cortices during follow-up in Patient P3. (b) MRI scans of the same patient

9   obtained in 2013 (left) and 2014 (right) showing stable appearance of white matter lesions. (c,

10   d, e) MRI scans acquired in 2014 (left) and in 2019 (right) of another patient (P7)

11   demonstrating progressive cortical atrophy and increased enlargement of lateral ventricles

12   (c), mild progression of white matter lesions adjacent to posterior horn of lateral ventricles

13   (d), and more pronounced atrophy of corpus callosum (e).

14

15   **Figure 3.** Bilateral calcification of the basal ganglia seen in Patient P3. No significant

16   progression of the calcification was observed between the two consecutive CT scans acquired
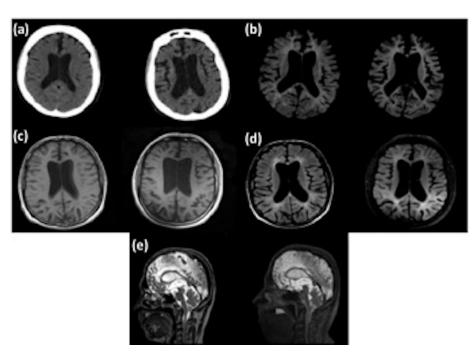
17   in 2012 (a) and 2017 (b).
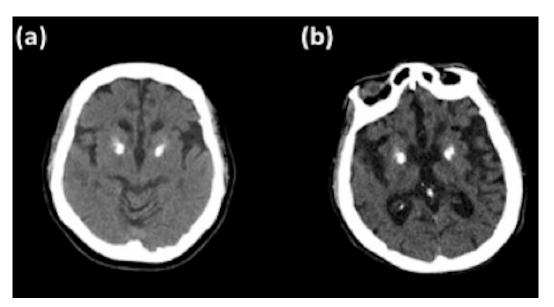
18

19   **Supplementary Figure.** Measurement of cortical thickness of Patient P9. Cortical thickness

20   was measured at a point 10 cm distal to the lesser trochanter. Cortical thickness index was

21   calculated as the ratio of the femoral diaphysis width (29.3 mm for this patient) minus

22   medullary canal width (11.1 mm for this patient) divided by femoral diaphysis width (29.3

23   mm for this patient) and found as 0.62.

ene_14908_f1.png

ene_14908_f2.png

ene_14908_f3.png